



This is a repository copy of *Vibrating tool path design for new multi-axial vibration assisted incremental sheet forming*.

White Rose Research Online URL for this paper:

<https://eprints.whiterose.ac.uk/id/eprint/231238/>

Version: Accepted Version

Proceedings Paper:

Chang, Z., Booth, J. and Long, H. orcid.org/0000-0003-1673-1193 (2024) Vibrating tool path design for new multi-axial vibration assisted incremental sheet forming. In: Mocellin, K., Bouchard, P.-O., Bigot, R. and Balan, T., (eds.) Proceedings of the 14th International Conference on the Technology of Plasticity - Current Trends in the Technology of Plasticity: ICTP 2023 - Volume 2. 14th International Conference on the Technology of Plasticity - Current Trends in the Technology of Plasticity (ICTP 2023), 24-29 Sep 2023, Mandelieu - La Napoule, France. Lecture Notes in Mechanical Engineering, 2. Springer Nature Switzerland, pp. 603-612. ISBN: 9783031409196. ISSN: 2195-4356. EISSN: 2195-4364.

https://doi.org/10.1007/978-3-031-40920-2_62

© 2023 The Authors. Except as otherwise noted, this author-accepted version of a paper published in Proceedings of the 14th International Conference on the Technology of Plasticity - Current Trends in the Technology of Plasticity: ICTP 2023 - Volume 2 is made available via the University of Sheffield Research Publications and Copyright Policy under the terms of the Creative Commons Attribution 4.0 International License (CC-BY 4.0), which permits unrestricted use, distribution and reproduction in any medium, provided the original work is properly cited. To view a copy of this licence, visit <http://creativecommons.org/licenses/by/4.0/>

Reuse

This article is distributed under the terms of the Creative Commons Attribution (CC BY) licence. This licence allows you to distribute, remix, tweak, and build upon the work, even commercially, as long as you credit the authors for the original work. More information and the full terms of the licence here: <https://creativecommons.org/licenses/>

Takedown

If you consider content in White Rose Research Online to be in breach of UK law, please notify us by emailing eprints@whiterose.ac.uk including the URL of the record and the reason for the withdrawal request.



eprints@whiterose.ac.uk
<https://eprints.whiterose.ac.uk/>

Vibrating Tool Path Design for New Multi-axial Vibration assisted Incremental Sheet Forming

Zhidong Chang, Jamie Booth and Hui Long*

Dept. of Mechanical Engineering, The University of Sheffield, Sheffield, UK

* h.long@sheffield.ac.uk

Abstract. In this study, a new multi-axial vibration assisted incremental sheet forming (MV-ISF) process is introduced by developing a vibrated toolpath and an ellipsoidal headed tool design. The process has been shown to improve the formability of tested materials due to the introduction of a low-frequency and high-amplitude vibration field. To understand the forming characteristics of the MV-ISF process, the geometrical accuracy, surface quality and formability in forming a conic geometry are investigated through experiments and finite element analysis using two aluminium alloys and compared with that formed using the conventional ISF tool path design. An analytical model of the material deformation under the vibration condition is also proposed to assess the enhanced formability of the MV-ISF process. The new vibrated tool path design combined with the use of the ellipsoidal headed tool provides a simple and potentially effective solution for improving the forming accuracy, surface quality and formability of ISF manufactured parts.

Keywords: Incremental Sheet Forming; Multi-axial Vibration; Tool Path Design.

1 Introduction

Incremental sheet forming (ISF) is considered as a flexible sheet metal forming process, potentially suitable for low volume production of customised sheet metal parts. Considerable studies have been conducted to investigate the deformation mechanisms of ISF process and its potential industrial applications. Investigation on the forming quality is of importance to address current issues of ISF parts, including geometrical accuracy, surface quality, and formability.

Vibration-assisted ISF (VAISF) process was proposed with the aim of improving the formability and surface quality in ISF. Vahdati et al. [1] firstly introduced the ultrasonic vibration into ISF process and demonstrated that the VAISF process had advantages in reducing the forming force, geometrical deviation and surface roughness, which was also validated by other studies in [2, 3]. The forming force was reduced significantly for the materials with higher yield stress, by adopting higher vibration energy and lower feed speed [4, 5]. Amini et al. [6] and Yang et al. [7] demonstrated that the use of ultrasonic vibration had a positive effect on improving the formability of sheet metals.

Amini et al. [8] reported a distinct improvement of surface hardness under the effect of ultrasonic vibration. Li et al. [9] developed a hybrid constitutive model to describe the material behaviour under VAISF condition. Different from the ultrasonic vibration with high frequency, Lu et al. [10] developed low-frequency and high amplitude vibrations in ISF process through the design of single- and double-offset on ellipsoidal headed tools under rotation. A hard-to-form material, magnesium alloy AZ31B, was processed and laminated ultrafine-grained structures were generated by these vibrating tools [10].

In addition to the formability studies of sheet materials, the improvement of forming quality has also been investigated. The ISF tool path design has shown significant effect on the forming quality. Filice et al. [11] proposed a spiral tool path to eliminate scratch marks on the part surface to improve the surface quality. Wang et al. [12] added an equal-diameter spiral path to the conventional helix tool path along circumferential direction to improve the forming limit of the sheet material. To avoid the biaxial tension condition using the conventional toolpath, Wen et al. [13] applied the multi-direction tool path, in which the moving direction of each contour kept changing. Lu et al. [14] developed a feature-based tool path through calculating the equi-potential contour lines to improve the geometrical accuracy and surface quality. Chang et al. [15] proposed a point-contact tool path to reduce the circumferential friction of the tool and showed the benefits in reducing geometrical deviation and improving formability of the material.

The vibration-assisted forming methods described above applied a unidirectional vibration field along the tool axis. However the ISF process involves three-dimensional stress states, the multi-axial vibration field using the tool path design can provide further improvement in forming quality but also maintain process flexibility.

In this work, a new multi-axial vibration assisted incremental sheet forming (MV-ISF) with a low-frequency and high-amplitude vibration field was proposed by creating a new vibrated tool path design and using an ellipsoidal headed tool. It is applied to form two materials of aluminium alloy sheets, AA5251-H22 and AA6082-T6. The effect of the new tool path design on the geometrical accuracy, surface quality and formability are investigated and compared with the conventional ISF (CISF) process. The influence of vibration amplitude on the formability and forming quality is investigated through experiments, an analytical model and finite element method.

2 Multi-axial Vibration Assisted ISF (MV-ISF)

To further improve the formability of sheet metal under vibration fields, the MV-ISF process is proposed with the flexible and controllable 3D vibration field through

combining a new vibrated tool path (VTP) with the use of the ellipsoidal headed tool. Different from the conventional ball head tool (T0), the ellipsoidal headed tool has an ellipsoidal head, named as T2, it exerts a radial vibration field with high amplitude and low frequency onto sheet metal, as shown in Fig. 1. In addition to the radial vibration caused by the ellipsoidal headed tool, an axial vibration is also applied to the sheet through employing a vibrated tool path. Employing this vibrated tool path, the forming tool moves up and down at a certain axial distance h while travelling along the circumferential direction of the conic part as shown in Fig. 1(c). This results in discontinuous contact between tool and sheet. The tool employing this new vibrating tool path thus introduces the axial vibration field into the sheet in MV-ISF process.

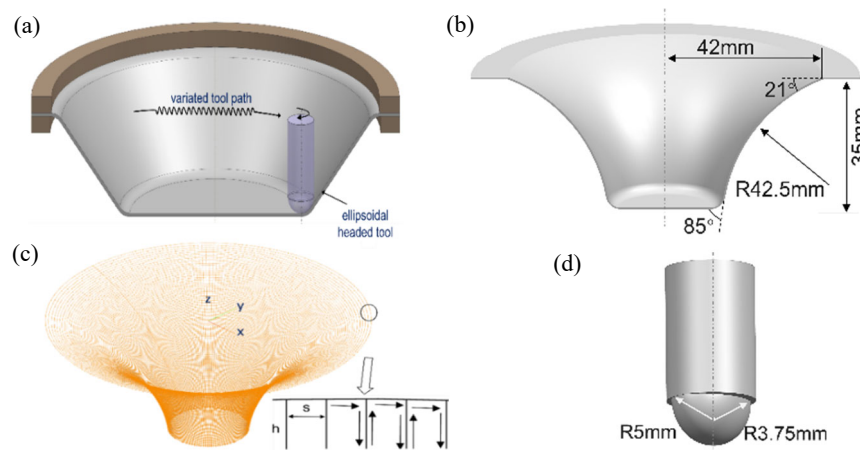


Fig.1. Illustration of the MV-ISF (a) schematic of the MV-ISF process; (b) conic part geometry; (c) vibrating tool path; (d) ellipsoidal headed tool.

3 Analysis of MV-ISF Experimental Results on Forming Quality

3.1 Geometrical accuracy

Fig.1 (b) shows the conical shape with varied wall angle formed in the experiment. To compare the difference of geometrical accuracy of the formed parts, Fig. 2 shows the measured part profiles along the cross section of the conic part using different tools and tool paths with step depth of 0.3mm using AA5251 with sheet thickness 1mm. The vibration tool path (VTP) with different axial distances ($h=0.1\text{mm}$ and 0.3mm) is adopted and compared with the conventional tool path (CTP).

As shown in Fig. 2, the part profiles using VTP show a considerably improved geometrical accuracy, especially for VTP with $h=0.3\text{mm}$. It is possible that the MV-ISF may reduce the residual stress by introducing both axial and radial vibration fields, which will be discussed in the following finite element analysis.

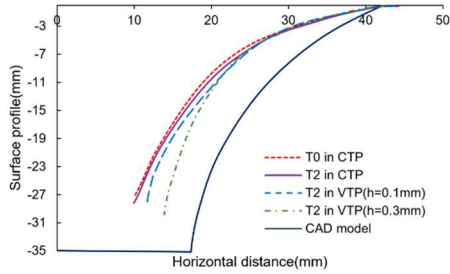


Fig. 2. Part profiles by using MV-ISF and CISF.

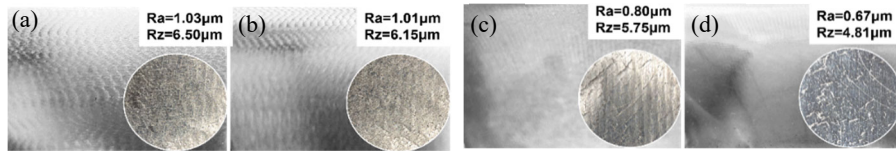


Fig. 3. Surface morphology by using MV-ISF and CISF: (a) T0 & CTP; (b) T2 & CTP; (c) T2 & VTP $h=0.1\text{mm}$; (d) T2 & VTP $h=0.3\text{mm}$.

3.2 Surface quality

Fig. 3 shows the surface morphology on the inner surface of the inclined wall of the conic part by different tools and tool paths. The surface is scanned by Alicona and the surface roughness is measured along the circumferential direction of the conic part. In the MV-ISF experiment, sufficient oil lubricant is used between tool and sheet. For the conic part produced by the CTP with tool rotation, a fish-scale texture can be seen on the surface as shown in Figs. 3(a) and (b), resulting in a reduced surface quality. By employing the VTP in MV-ISF, the surface quality is improved with reduced surface roughness and no obvious fish-scale texture can be observed on the sheet surface, as shown in Figs. 3(c) and (d). It is worth noting that by using the VTP with $h=0.3\text{mm}$, the inner surface of the part as shown in Fig. 3(d) has achieved a smoother surface finishing which is difficult to achieve using conventional ISF processes. This is because by using the VTP, the fish-scale surface texture is repeatedly flattened by the forming tool under the action of the axial vibration field, thus achieving the improved surface quality.

3.3 Forming limit

To investigate the formability, conical parts using AA5251 and AA6082 sheets are produced by employing different tools and tool paths. The thickness strain are obtained

by measuring the sheet thickness at the fracture, and the fracture strain is calculated based on the assumptions of volume constancy and plane strain condition [16]:

$$\bar{\varepsilon}_f = \frac{2}{\sqrt{3}} \ln \frac{t_0}{t} \quad (1)$$

where t_0 is the original thickness, and t is the measured thickness.

Fig. 4 shows an increased maximum thinning and fracture strain by the MV-ISF, when compared with that by the CTP. The fracture strain by VTP $h=0.1\text{mm}$ is 8.6% higher than that by the CISF for AA5251 and 23% higher for AA6082. Compared with using T0 and the CTP, the fracture strain by using T2 and VTP $h=0.3\text{mm}$ is increased by 28.1% for AA5251 and 16.1% for AA6082. Therefore, the sheet formability can be effectively improved by the developed MV-ISF process. It is widely recognised that the application of a vibration field can reduce the dislocation density of the sheet metal thus improving the formability. The dislocation density of AA6082, with a higher strength, is significantly higher than that of AA5251, therefore the volume effect caused by the vibration field is more obvious in AA6082, leading to the greater decreasing of dislocation density and significant improvement of formability compared with AA5251.

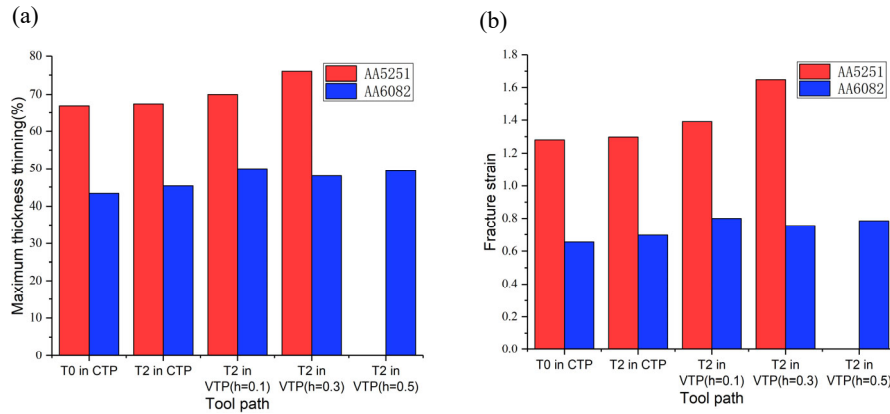


Fig. 4. Formability by using CTP and VTP: (a) sheet thinning; (b) fracture strain.

4 Analytical Model of Estimating Stress Reduction in MV-ISF

To investigate the effect of vibration field on the material plastic deformation, vibration amplitude and frequency generated by different tools and tool paths are measured by using an Eddy current sensor, with the highest measurement accuracy of $0.01\mu\text{m}$, to obtain the displacement of the sheet. When the tool contacts the sheet measurement

point where the sensor is located, elastic-plastic deformation of the sheet is measured by displacement, as shown in Fig. 5. The fluctuations of displacement are considered being caused by the vibration field. The axial fluctuation due to the VTP will cause a reduction of feed rate and an increase of forming time. As shown in Fig. 5(a) and Fig. 5(b), in the same time period, the tool by the CTP contacts the sheet measurement point three times, while using the VTP the tool only contacts the sheet once, indicating an increase of forming time by using the VTP.

After applying Fourier processing of the measured displacement data in Fig. 5(c), the vibration amplitude and frequency of the sheet in the MV-ISF are obtained, as shown in Fig. 5(d). The MV-ISF process creates both axial and radial vibration fields, leading to a higher frequency. No obvious difference of radial vibration amplitude is observed by using different tool paths, but the axial amplitude by the VTP increases significantly, as shown in Fig. 5(d). The maximum amplitudes of CTP and VTP ($h=0.1\text{mm}$) are $25\mu\text{m}$ and $32.6\mu\text{m}$ respectively, while the amplitude generated by the VTP ($h=0.3\text{mm}$) is measured as $87.2\mu\text{m}$, which is much greater than other process conditions tested.

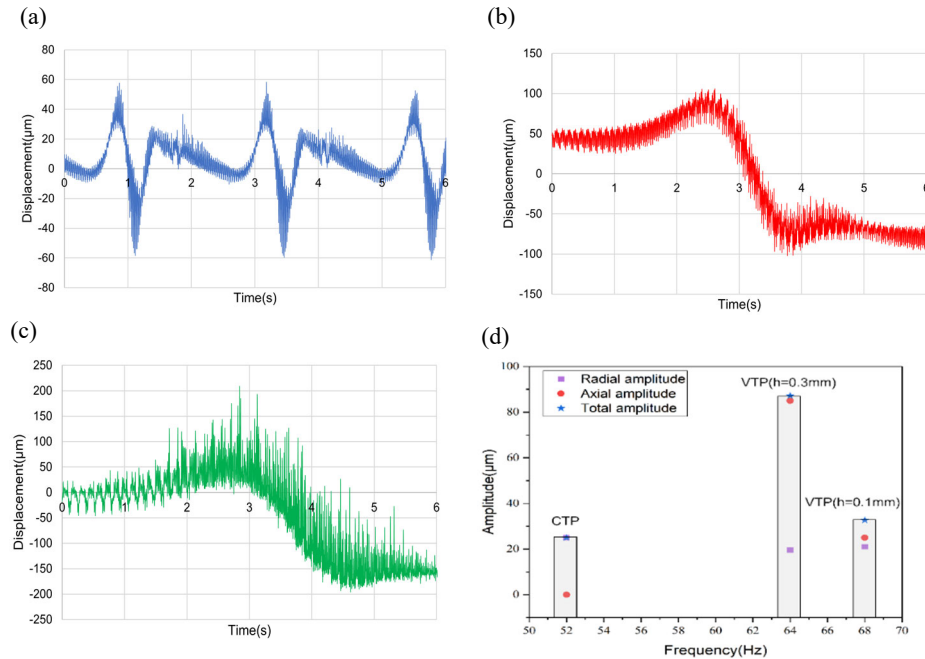


Fig. 5. Vibration measurements by using different tool paths: (a) T2 & CTP; (b) T2 & VTP $h=0.1\text{mm}$; (c) T2 & VTP $h=0.3\text{mm}$; (d) Vibration amplitude and frequency.

It has been reported that the vibration field shows significant effect on the material deformation, which can be explained by vibration softening, stress superposition and friction reduction. In this work, the stress reduction $\Delta\sigma$ caused by the large-amplitude vibration field is described as a combined effect of vibration softening and stress superposition as shown in Fig. 6(a), which can be expressed as

$$\Delta\sigma = \Delta\sigma_{su} + \Delta\sigma_{so} \quad (2)$$

where $\Delta\sigma_{so}$ and $\Delta\sigma_{su}$ is the stress reduction due to vibration softening and stress superposition respectively. As an important factor related to the stress reduction in the MV-ISF, the stress superposition maintains an exponential relationship with vibration amplitude as investigated by Wang et al. [17] as

$$\Delta\sigma_{su} = -K\xi^n \quad (3)$$

where K and n are the hardening exponent and material strength coefficient of the material. Based on thermal activation theory, the stress reduction due to the stress softening is considered to be related to the vibration energy density [17]

$$\Delta\sigma_{so} = -\beta M \hat{\tau} (E / \hat{\tau})^m \quad (4)$$

where $\hat{\tau}$ is the mechanical threshold of the sheet material and E is the vibration energy density; β and m are the material parameters obtained from experiments, and M is the Taylor factor, which is taken as 3.06. It is considered that the vibration energy density E in the MV-ISF process maintains a positive relationship with the vibration amplitude and frequency. When the ellipsoidal tool rotates, its vibration energy density along radial direction can be calculated by

$$E_h = J\omega^2 = \frac{1}{5}\xi_h^2\omega^2\rho \quad (5)$$

The axial vibration energy exerted by the VTP can be obtained by

$$E_v = \frac{1}{2}\xi_v^2\omega^2\rho \quad (6)$$

where ξ_v and ξ_h are vibration amplitude along axial and radial direction, respectively; while ω and ρ are the vibration frequency and density of the material. The total energy density caused by vibration field in the MV-ISF process can be obtained by

$$E = E_v + E_h = \left(\frac{1}{2}\xi_v^2 + \frac{1}{5}\xi_h^2\right)\omega^2\rho \quad (7)$$

Fig. 6 shows the calculated stress reduction using different tool paths by the developed analytical model in Eqs. (3) and (4). The values of vibration amplitude and frequency

used in the analytical model are from the experimental results in Fig. 5(d). The material parameters of AA5251 are: $\rho=2700\text{kg/m}^3$, $\hat{\tau}=138\text{MPa}$, $\beta=15$, $m=0.5$, $K=389$, $n=0.228$. Higher stress reduction contributes to the improvement of formability. As shown in Fig. 6, the stress superposition effect shows no obvious difference between processes, but the calculated stress reduction due to vibration softening increases with the increase of the axial distance h and vibration energy in the VTP, which is consistent with the improvement of fracture strain shown in Fig. 4. Therefore, the analysis of stress reduction indicates that the improved formability of the MV-ISF is due to the effect of the axial vibration field and the increasing of vibration energy by the VTP.

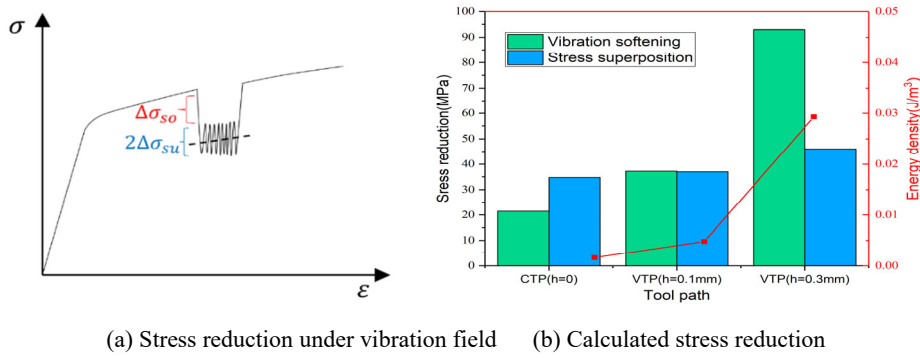


Fig. 6. Comparison of stress reduction by using different ISF processes.

5 Finite element analysis

In order to understand the mechanism leading to the improved geometrical accuracy in the MV-ISF, finite element (FE) models of forming the conic part using different tool paths, shown in Fig. 1, are developed by using FE software ABAQUS to simulate the MV-ISF process. AA5251 material and shell elements using five integral points through thickness are selected in the simulation models using von Mises yield criterion. The coefficient of friction is assumed to be 0.05 in the simulation, taken from Eyckens et al. [18]. For a conventional ISF process, the sheet deformation is plane strain state [19], but it is essential to confirm whether the MV-ISF changes the deformation state. Fig. 7(a) shows the strain paths obtained from both MV-ISF and CISF processes. It is clear that the minor strain is small when compared with the major strain in the MV-ISF. Therefore the deformation using the VTP and ellipsoidal headed tool in the MV-ISF is still in the plane strain state. The MV-ISF process can increase the fracture strain through introducing the vertical vibration field without changing the deformation state.

The simulated result in Fig. 7(b) shows that the stress triaxiality at contact area decreases cyclically under the effect of the vibration field, and the fluctuation of stress triaxiality is related to the vibration amplitude. The greater variation ranges of stress triaxiality in the MV-ISF provides a valid explanation for the improved formability of the material in the MV-ISF when compared with that in the CISF.

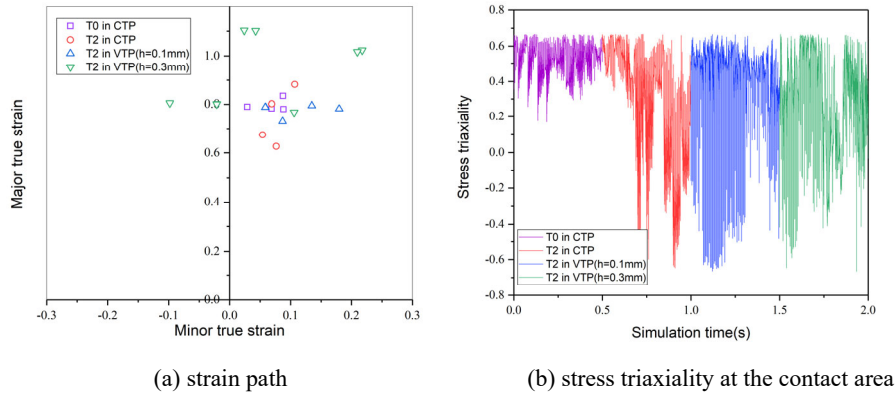


Fig. 7. Simulation results using different processing methods CISF and MV-ISF.

Fig. 8 compares the residual von Mises stress distribution under CISF and MV-ISF. The average residual stress using the VTP is obviously smaller than that using the CTP, and the maximum residual stress by the VTP is about 580MPa, which is smaller than that by the CTP of 650MPa. It is shown that the decreased residual stress using the VTP is caused by the axial vibration field, and the internal residual stress is released during cyclic loading and unloading in the MV-ISF. Through releasing the residual stress, the springback of a formed part decreases which contributes to the improvement of geometrical accuracy. Based on the above simulated results of the residual stress, it can be concluded that the MV-ISF process can improve the geometrical accuracy of the formed part as shown in Fig. 2 as a result of releasing the residual stress due to vibration.

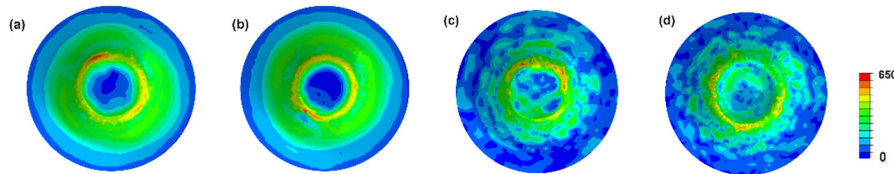


Fig. 8. Finite element simulation of residual stress distribution (MPa): (a) T0 & CTP; (b) T2 & CTP; (c) T2 & VTP $h=0.1\text{mm}$; (d) T2 & VTP $h=0.3\text{mm}$.

6 Conclusions

In this study, a new MV-ISF process is proposed by introducing axial and radial vibration fields in ISF through employing a vibrated tool path design combined with the use of the ellipsoidal headed tool. Experiments using AA5251 and AA6082, analytical modelling and finite element simulations have been conducted to investigate the improvement of the new process in geometrical accuracy, surface quality and formability. The main conclusions are:

- The MV-ISF process can significantly improve the fracture strain through increasing the vibration energy and decreasing the stress triaxiality under the effect of the exerted axial vibration field. This new vibrating tool path design provides a simple and feasible solution for improving the material formability.
- The new MV-ISF shows its advantage in decreasing the geometrical deviation of the formed part by releasing the residual stress due to the effect of the vibrated tool path.
- Increasing the axial distance in the vibrated tool path of the MV-ISF improves geometrical accuracy, surface quality and formability of formed parts.

Acknowledgments

The authors wish to acknowledge the funding support received from the UK EPSRC (Engineering and Physical Sciences Research Council) through project grants EP/W010089/1 and EP/T005254/1.

References

1. Vahdati M, Mahdaviinejad R, Amini S. (2015) Investigation of the ultrasonic vibration effect in incremental sheet metal forming process. *Proc. Inst. Mech. Eng. Pt. B: J. Eng. Manuf.* 231: 971–982.
2. Mingshun Y, Lang B, Yunbo L, et al. (2019) Research on the radial accuracy of ultrasonic VA single point incremental forming parts. *Int. J. Aerosp. Eng.* 1–9.
3. Cheng Z, Li Y, Li J, et al. (2022) Ultrasonic assisted incremental sheet forming: Constitutive modeling and deformation analysis. *Journal of Materials Processing Tech.* 299: 117365.
4. Long Y, Li Y, Sun J, et al. (2018) Effects of process parameters on force reduction and temperature variation during ultrasonic assisted incremental sheet forming process. *Int. J. Adv. Manuf. Technol.* 97:13–24.
5. Bai L, Li Y, Yang M, et al. (2019) Modeling and analysis of single point incremental forming force with static pressure support and ultrasonic vibration. *Materials* 12:1899.
6. Amini S, Hosseinpour Gollo A, Paktinat H. (2016) An investigation of conventional and

- ultrasonic-assisted incremental forming of annealed AA1050 sheet. *Int. J. Adv. Manuf. Technol.* 90: 1569–1578.
7. Yang M, Bai L, Li Y, et al. (2019) Influences of vibration parameters on formability of 1060 aluminum sheet processed by ultrasonic VA single point incremental forming. *Adv. Mater. Sci. Eng.* 1–12.
 8. Amini S, Nazari F, Baraheni M, et al. (2018) Investigating the effect of rotation speed and ultrasonic vibrations in the incremental forming process. *Int. J. Adv. Design Manuf. Technol.* 11: 91–97.
 9. Li Y, Chen X, Sun J, et al. (2017) Effects of ultrasonic vibration on deformation mechanism of incremental point-forming process. *Procedia Engineering* 207: 777–782.
 10. Lu B, Li Z, Long H, et al. (2017) Microstructure refinement by tool rotation-induced vibration in incremental sheet forming. *Procedia Engineering* 207: 795–800.
 11. Filice L, Fratini L, Micari F. (2002) Analysis of Material Formability in Incremental Forming, *CIRP Ann -Manuf Technol* 51:199-202.
 12. Wang J, Li L H, Zhou P, et al. (2018) Improving formability of sheet metals in incremental forming by equal diameter spiral tool path, *Int J Adv Manuf Technol* 89:3527-3534.
 13. Wen T, Chen X, Zheng J, et al. (2017) Multi-directional incremental sheet forming-a novel methodology for flexibly producing thin-walled parts, *Int J Adv Manuf Technol* 91:1909-1919.
 14. Lu B, Chen J, Ou H, et al. (2013) Feature-based tool path generation approach for incremental sheet forming process, *J Mater Process Technol* 213:1221–1233.
 15. Chang Z, Huang W, Li M, et al. (2020) A new tool path with point contact and its effect on incremental sheet forming process, *Int J Adv Manuf Technol* 110:1515-1525.
 16. Lu B, Fang Y, Xu D K, et al. (2014) Mechanism investigation of friction-related effects in single point incremental forming using a developed oblique roller-ball tool, *Int J Mach Tools Manuf* 85:14-29.
 17. Wang C J, Liu Y, Guo B, et al. (2016) Acoustic softening and stress superposition in ultrasonic vibration assisted uniaxial tension of copper foil: Experiments and modeling, *Materials and Design* 112: 246–253.
 18. Eyckens P, Belkassam B, Henrard C, et al. (2011) Strain evolution in the single point incremental forming process: digital image correlation measurement and finite element prediction, *Int J Mater Form* 4:55–71.
 19. Silva M, Skjoedt M, Martins P, et al. (2008) Revisiting the fundamentals of single point incremental forming by means of membrane analysis. *Int J Mach Tools Manuf* 48:73-83.